Available online at www.sciencedirect.com
ScienceDirect
Journal of Magnetism and Magnetic Materials 320 (2008) 1639–1644
Journal of magnetism and magnetic materials
www.elsevier.com/locate/jmmm

FINEMET type alloy without Si: Structural and magnetic properties

D. Muraca[a,*], V. Cremaschi[a,b], J. Moya[a,b], H. Sirkin[a,b]

[a]*Instituto de Tecnologías y Ciencias de la Ingeniería Hilario Fernández Long, Facultad de Ingeniería, UBA-CONICET, Paseo Colón 850, (1063) Buenos Aires, Argentina*
[b]*Member of Carrera del Investigador, CONICET, Argentina*

Received 28 December 2007; received in revised form 15 January 2008
Available online 24 January 2008

Abstract

Magnetic and structural properties of a Finemet type alloy ($Fe_{73.5}Ge_{15.5}Nb_3B_7Cu_1$) without Si and high Ge content were studied. Amorphous material was obtained by the melt spinning technique and was heat treated at different temperatures for 1 h under high vacuum to induce the nanocrystallization of the sample. The softest magnetic properties were obtained between 673 and 873 K. The role of Ge on the ferromagnetic paramagnetic transition of the as-quenched alloys and its influence on the crystallization process were studied using a calorimetric technique. Mössbauer spectroscopy was employed in the nanocrystallized alloy annealed at 823 K to obtain the composition of the nanocrystals and the amorphous phase fraction. Using this data and magnetic measurements of the as-quenched alloy, the magnetic contribution of nanocrystals to the alloy annealed at 823 K was estimated via a linear model.

PACS: 75.50.Tt; 81.07.b 75.75.+a; 61.46.w

Keywords: Nanocrystalline materials; Magnetic structure; FINEMET ribbon; Melt spinning; Macroscopic and atomistic magnetization analysis

1. Introduction

Over the past few decades, nanocrystalline magnetic materials have been investigated for applications in magnetic devices that require soft magnetic materials such as transformers, inducted devices, magnetic shielding, etc. The benefits found in the nanocrystalline alloys stem from their chemical and structural variation on a nanoscale, which is important for developing optimal magnetic properties.

Nanocrystalline alloys can be described as $TL_{(1-x)}[TE, M, NM]_x$ where TL denotes a late ferromagnetic transition metal element, TE is an early transition metal element, M is a metalloid, and NM is a noble metal. x is usually less than 0.20 i.e. with as many late ferromagnetic transition metals (TL = Co, Ni, or Fe) as possible. The remaining early transition metals (TE = Zr, Nb, Hf, Ta, etc.) limit the grain growth and metalloids (M = B, P, etc.) promote glass formation in the precursor. The noble metal elements (TN = Cu, Ag, Au) serve as nucleating agents for the ferromagnetic nanocrystalline phase. The compositions are limited by the glass formation ability of the alloy prior to the nanocrystallization route. These alloys can be considered two phase materials with a nanocrystalline ferromagnetic phase and a residual amorphous phase between the grains. These materials have relatively high resistivity and low magnetocrystalline anisotropy. These properties make nanocrystalline alloys adequate candidates to be used as soft magnetic materials. The FINEMET ($Fe_{73.5}Si_{13.5}Nb_3B_9Cu_1$) [1], NANOPERM ($Fe_{88}Zr_7B_4Cu_1$) [2,3] and HITPERM ($Fe_{44}Co_{44}Zr_7B_4Cu_1$) [4] nanocrystalline alloys are the softest magnetic materials developed to date and are currently being considered for various commercial applications.

In particular FINEMET alloy exhibits excellent soft magnetic properties such as high permeability ($\mu_r \sim 10^5$ at 1 kHz), low saturation magnetostriction ($\lambda \sim 2 \times 10^{-6}$), relatively high saturation magnetization ($B \sim 1.2$ T) and resistivity ($\rho \sim 115\,\mu\Omega\,cm$) and a very low average structural anisotropy ($\langle K \rangle \sim 5\,J/m^3$) [1,5]. A typical nanocrystalline microstructure grows when the amorphous alloy is

*Corresponding author. Tel.: +54 11 43430891.
E-mail address: diego.muraca@gmail.com (D. Muraca).

0304-8853/$ - see front matter © 2008 Elsevier B.V. All rights reserved.
doi:10.1016/j.jmmm.2008.01.034

crystallized by the primary crystallization process at nearly 823 K, forming BCC α-Fe(Si) nanocrystals (50–80 vol% of the alloy [5]) with grain sizes of about 10–15 nm surrounded by a ferromagnetic amorphous matrix. This microstructure exhibits excellent soft magnetic properties that are attributed to the reduction in the effective magnetic anisotropy, which is randomly averaged out by the exchange interaction. Hence the condition to obtain such soft magnetic properties is that the structural correlation length should be shorter than the magnetic exchange correlation length [5].

Several works have studied the influence of different elements on these alloys [6–10] and the state of the art has been reviewed in different works [5,11,12]. In this paper we investigated the influence of the replacement of all Si and part of B with Ge in the FINEMET type alloy.

2. Experimental

A FINEMET type ribbon $Fe_{73.5}Ge_{15.5}Nb_3B_7Cu_1$ (Ge15.5) was obtained using the melt spinning technique. Nanocrystallization was achieved by annealing the sample at different temperatures (T_{ann}) under vacuum in the range between 673 and 873 K for one hour. The structural evolution of the alloy was followed by X-ray diffraction (XRD) using monochromatized Cu Kα radiation ($\lambda = 1.5406$ Å) in a Rigaku diffractometer and thermal evolution was studied by differential scanning calorimetry (DSC) using a Perkin-Elmer DSC-PYRIS 1 at different scanning rates (10, 20, 40 and 80 K/min). Magnetic saturation of the samples was measured in a Physical Property Measurement System (PPMS) at room temperature at a maximum applied field of 9 T. Coercivity was obtained from the hysteresis loops measured on both as-quenched and annealed open strips (10–12 cm long) using a quasi-static fluxmetric method by applying an axial field on the sample and collecting the induced signal in a secondary compensated pick-up coil. Mössbauer spectroscopy (MS) (^{57}Co source in a Rh matrix in transmission geometry at room temperature) was performed to study the structure of the sample in the optimal magnetic state. Mössbauer spectrum was fitted employing the NORMOS program [13].

3. Results and discussion

3.1. Structural

The nanocrystalline BCC α-Fe(Si) phase typically forms in FINEMET alloys, with a DO_3 structure [14]. In our study all the Si and 2 at% of B were replaced with Ge so we expected that Ge would take the place of Si, as previously reported by Moya et al. [15]. Fig. 1 shows the XRD patterns of the amorphous sample and the samples annealed at different temperatures.

It can be seen that the nanocrystallization of α-Fe(Ge) begins at $T_{ann} = 673$ K and no borides precipitate even at

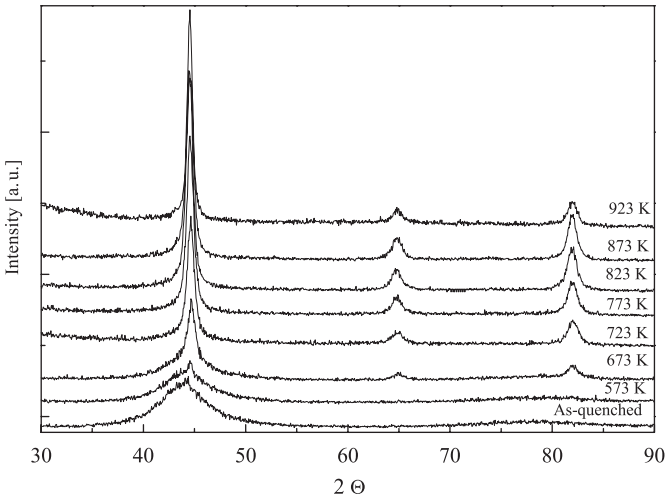

Fig. 1. XRD patterns corresponding to samples annealed at different annealing temperatures.

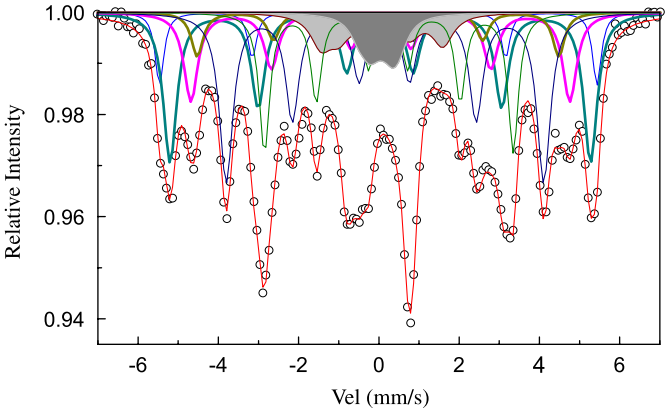

Fig. 2. Mössbauer fitted spectrum of the alloy annealed at 823 K. The shadowed subspectra correspond to the amorphous phase.

$T_{ann} = 923$ K, differing from typical FINEMET alloys [16,17]. In agreement with previous reports [18], this result suggests that Ge stabilizes the nanocrystalline phase and delays boride precipitation.

The lattice parameter, a, of the Ge15.5 nanocrystalline alloy annealed at 823 K ($a = 5.764$ Å) is larger compared with the FINEMET alloy ($a = 5.676$ Å, [15]) due to the difference in atomic size between Ge and Si.

Fig. 2 shows the Mössbauer fitted spectrum of the alloy annealed at 823 K. The spectrum was fitted employing two (wide) sextets for the amorphous phase (hyperfine magnetic field, Bhf = 3.07 and 9.41 T, respectively) plus other six for the crystalline interactions.

Some of the crystalline hyperfine interactions parameters are given in Table 1. Perhaps the most interesting feature of these results is that the amount of Fe atom fraction obtained by the MS fits in the amorphous phase is about 12.3%. If we compare this value with those obtained by the same technique for typical FINEMET alloy (i.e. around 40% [15,19,20]) the former is markedly lower. This is due to two reasons: a low boron content (independent of Ge content) as compared with the 9 at% of traditional FINEMET [5] and a

Table 1
Isomer shift (δ), magnetic hyperfine interaction (Bhf), and relative resonant absorption area (RA) obtained from the Mössbauer fitted spectrum corresponding to the alloy annealed at 823 K

Spectrum	δ (mm/s)	Bhf (T)	RA (%)	Fe-sites
1	−0.00738	33.75	6.7620	$A_0 + D_0$
2	0.03064	32.45	24.7618	$D_1 \rightarrow D_6$
3	0.04576	29.5	15.2121	A_1
4	−0.02117	27.9	6.41319	A_2
5	0.1432	24.51	28.0059	A_3
6	0.24091	19.2028	17.9308	A_4

high Ge content. In a previous work Moya et al. [15] observed that substitution of Ge by Si in FINEMET type alloys produce an increment of the crystalline fraction. In the present case the increment in crystalline fraction compared with FINEMET is nearly 50%.

In order to calculate the Ge content in the nanocrystals we employed the binomial distribution method for the DO_3 structure [14]. The ordered DO_3 structure exists between about 12.5 and 31 at% Si and consists of two sublattices: one with eight Fe atoms (named A) and the other with Fe and Si atoms (Ge in our case, named D). The A_n, D_n are binomial distributions used to calculate the Ge content. $A_n = A(n,0)$ represents an iron atom in the A sublattice (eight Fe atoms) having n Ge atoms as nearest neighbors and 0 Ge atoms as next nearest neighbors. $D_n = D(0,n)$ represents an iron atom in the D sublattice ((8-n) Fe and n Ge atoms) having n Ge atoms as next nearest neighbors and 0 Ge atoms as nearest neighbors. Based on RA data and the binomial distributions, the atomic percentage concentration of Ge in the nanocrystals was calculated to be 18.6 ± 0.5. This value is lower than that expected for a nominal as quenched composition of 15.5 Ge at%. This is a consequence of the high crystallization fraction present in this nanocrystalline alloy that on one hand reduces the amount of Ge in the nanocrystals and, on the other hand, impoverishes the amorphous phase in Fe obtaining a composition of the amorphous phase of ~44 at% Fe.

Different DSC heating rates were performed to analyze the ferromagnetic-paramagnetic transition (T_c) of the amorphous phase, the α-Fe(Ge) primary crystallization peak and its activation energy (E_a). The 40 K/min DSC curves of the studied alloy and the FINEMET one are plotted in Fig. 3a. It can be clearly seen that Ge tends to diminish the temperature of primary crystallization (T_{x1}) and delays the secondary crystallization corresponding to borides precipitation. Fig. 3b shows DSC curves of the alloy at different scanning rates (10, 20, 40 and 80 K/min).

The E_a of the alloy was obtained by using Kissinger and multiple scanning methods (MSM) [21,22].

The Kissinger method is based on the following equation:

$$\ln \frac{\beta}{T_p^2} = \frac{E_a}{RT} + C, \tag{1}$$

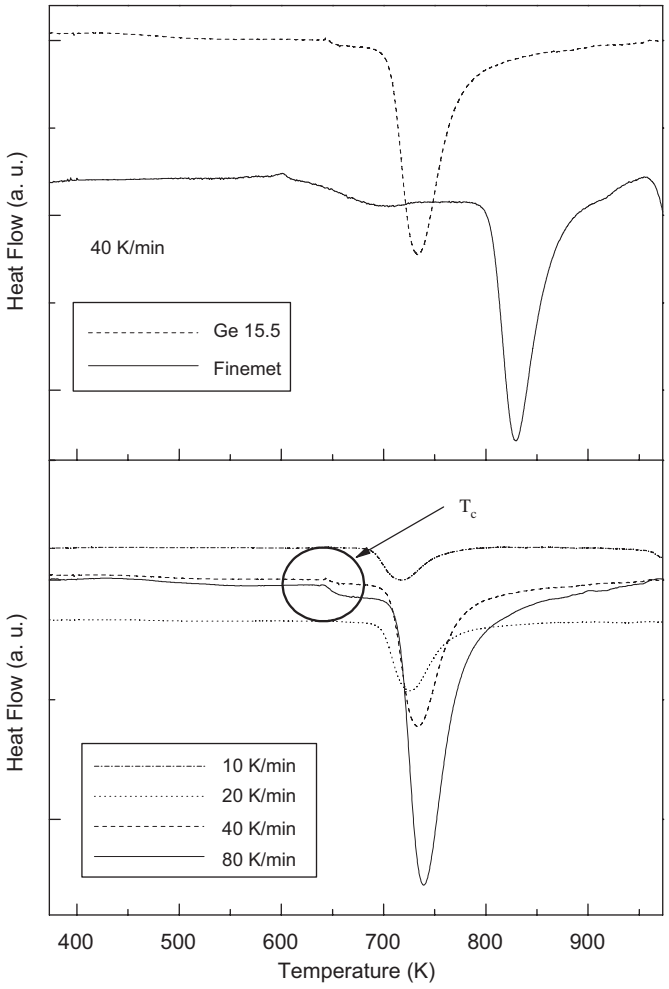

Fig. 3. (a) DSC curve of the studied alloy compared with the FINEMET alloy. (b) DSC curves of the alloy at different scanning rates (10, 20, 40 and 80 K/m).

where β is the heating rate, R is the universal gas constant, T is the temperature T_p is the peak temperature and C is a constant. Thus, E_a can be obtained from the slope of a straight line.

Taking into consideration the Arrhenius law for the reaction rate, the following equation can be obtained:

$$\ln\left(\frac{\partial x}{\partial t}\right) = \frac{E_a}{RT} + C, \tag{2}$$

where x is the nanocrystallized fraction and $\partial x/\partial t$ is the transformation rate. This last equation gives us a second method (MSM) to calculate E_a from the slope of the straight line when plotting $\ln(\partial x/\partial t)$ as a function of $1000/T$.

Fig. 4 shows the E_a values calculated using the multiple scanning method. A range of possible E_a values of the studied sample was observed in this case. These differences can be appreciated when analyzing the lowest and highest values of the nanocrystalline fraction and may be the result of the different growth processes which involve different activation energies. At the first stage of crystallization kinetics is controlled by the interface while in a second

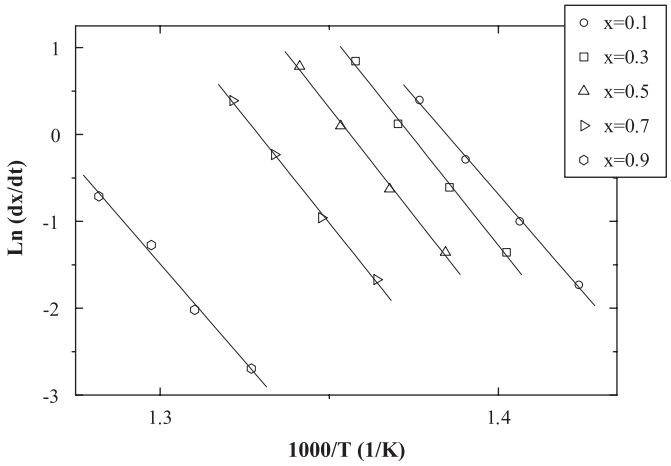

Fig. 4. Multiple scanning method of the alloy considering the crystalline fraction.

stage, kinetics is controlled by diffusion mechanisms in the amorphous matrix [7]. These two mechanisms can be intuitively observed in the asymmetric profile of the DSC curves. Table 2 summarizes different values obtained from DSC analysis of the alloy compared with values corresponding to FINEMET.

3.2. Magnetic

The magnetic softness of these materials is due to the fact that the structural correlation length is shorter than the magnetic exchange correlation length over which spins are coupled via exchange interaction.

The coercitivity can be associated to the mean value of the anisotropy as

$$H_C = \frac{p_c \langle K \rangle}{\mu_0 M_s}, \tag{3}$$

where p_c is a constant less than 1, μ_0 is the vacuum magnetic permeability, M_s is the saturation magnetization and $\langle K \rangle$ is the average value of the anisotropies that determine the magnetic behavior of the alloy. This value is controlled by the different magnetic and structural correlation lengths, and stresses induced in the material. The effective averaged value of the anisotropy can be expressed in a general form as

$$\langle K \rangle = \langle K_u \rangle + \langle K_1 \rangle, \tag{4}$$

where $\langle K \rangle$ is the averaged induced stress anisotropy and $\langle K \rangle$ is the averaged magnetocrystalline anisotropy.

Fig. 5 shows the H_c as a function of the annealing temperature. The graph was divided into three fundamental regions according to the microstructure of the material. In the first region (Region I) the material is essentially amorphous and the coercivity is determined by the induced stress in the material. Thus, the mean value of the anisotropies can be expressed as

$$\langle K_u \rangle = \tfrac{3}{2}\lambda \langle \sigma \rangle, \tag{5}$$

Table 2
T_c, T_{onset}, and T_p obtained from DSC data at 40 K/min and E_a calculated using two methods: multiple scanning (MSM) and Kissinger

	T_c	T_{onset}	T_p	E_a (eV/at)
FINEMET	593.0	796.2	829.7	4.30 [7]
Ge15.5	664.0	700.0	774.0	4.20±0.30 (MSM)/ 4.28 (Kissinger)

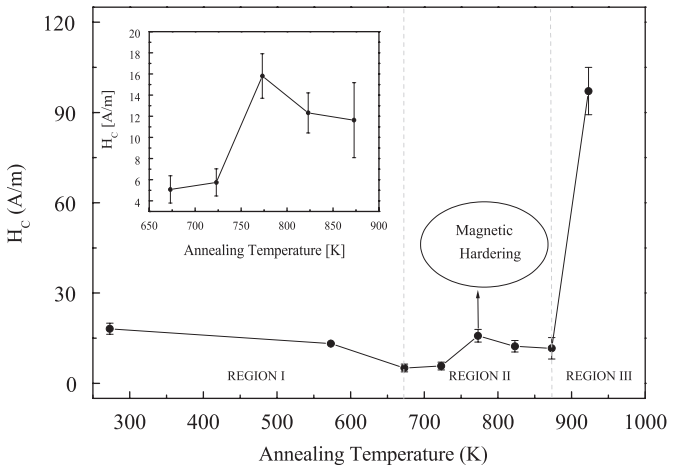

Fig. 5. Coercivity as a function of annealing temperature. Inbox: region where the alloy presents the optimal magnetic properties.

where $\langle \sigma \rangle$ is the average value of the residual stresses and λ is the saturation magnetostriction constant of the amorphous phase. $\langle \sigma \rangle$ tends to diminish during the heat treatment before primary crystallization. This behavior was observed in the alloy between the as-quenched sample and the sample treated at 673 K.

In the second region, between 673 and 873 K (Region II), the material presented the softest magnetic properties. Neglecting the effect of induced stresses in the material the magnetic behavior can be expressed in terms of the random anisotropy model [23]. The average crystalline anisotropies depend on grain size, D, crystallite anisotropy, K_1, and exchange stiffness values, A, as

$$\langle K_1 \rangle \approx \frac{K_1^4 D^6}{A^3}. \tag{6}$$

In most of these alloys magnetic hardening appears during the first stage of crystallization. This magnetic hardening was attributed to the fact that the very small crystallites act as inclusions which induce stresses that give rise to domain wall pinning centers in the amorphous matrix. Magnetic hardening of the alloy was observed at annealing temperatures close to 773 K.

In the last region (Region III), the structural correlation length is greater than the magnetic correlation length. This generates the magnetic hardness of the material, as can be observed in Fig. 5. Saturation magnetization of the sample was measured for the as-quenched and nanocrystalline state ($T_{ann} = 823$ K). The obtained values were

138 ± 2 emu/g for the as-quenched alloy and 140 ± 4 emu/g for the annealed sample. Taking into account that the amount of Fe was 72.66 wt% the magnetic moment per Fe atom in the amorphous alloy was $1.91 \pm 0.05\,\mu_B$/at.

The magnetic contribution of the nanocrystals in the alloy was calculated considering the Ge concentration in the crystallites (18.6 ± 0.5%) obtained by Mössbauer analysis. To obtain the magnetic contribution we used a simple and linear model which relates the change in the magnetic moment of the nanocrystals due to the addition of Ge in the cell. This model was first employed by Okumura et al. [24] in Si rich FINEMET alloys and it is based on experimental measurements performed on different alloys [25]. A detailed description of the model was published elsewhere [26].

The relationship between the amount of Ge atoms in the cell and the magnetic moment of an iron atom is given by:

$$\mu = \mu_0 + \kappa_{Ge} x_{Ge}, \tag{7}$$

where $\mu_0 = 2.15\,\mu_B$/at is the magnetic moment of an Fe atom in the absence of Ge as nearest neighbors (NN) in the BCC lattice, $v_{Ge} = -1.35\,\mu_B/\text{at}^2$ is the proportional constant of Ge [Corb], and x_{Ge} is the fraction of Ge atoms as NN in the cell on the basis of a total of 9 atoms. The κ_{Ge} constant is related with the change in the density of conduction electrons due to the expansion or contraction of the lattice and to the electronic configuration of the different atoms.

The magnetic moment of a cell can be expressed as $\mu_{cell} = \sum_i \alpha_i \mu_i$ with $\sum_i \alpha_i = \langle n_{Fe} \rangle$, where the α_i coefficients can be obtained from the concentration of Ge and Fe in the DO_3 structure with i from 1 to 4, and where $\langle n_{Fe} \rangle$ is the average number of iron atoms in the DO_3 cell and μ_i ($i = 2, 3$) is the magnetic contribution of an iron atom with i different number of Ge atoms as first neighbor in the BCC lattice.

In our case, the DO_3 structure of the nanocrystalline phase of the alloy has 18.6 at% Ge which means that there is an average of 13.024 Fe atoms and 2.276 Ge atoms in a unit cell, i.e. 122 out of 125 unit cells have 13 Fe and 3 Ge atoms and 3 out of 125 have 14 Fe atoms and 2 Ge atoms. We can consider that the 122/125 cells of the DO_3 structure with 13 Fe and 3 Ge atoms contain 5 Fe atoms with no Ge atoms as NN and 8 Fe with 3 Ge atoms as NN. The 5 first Fe atoms contribute to the magnetic moment per iron atom with $5x\mu_0$ and the last 8 Fe atoms contribute with $8x\mu_3$, where $\mu_3 = 1.7\,\mu_B$/at. Applying this same procedure to the 3/125 DO_3 cell with 14 Fe and 2 Ge atoms there are 6 Fe atoms with no Ge atoms as NN, resulting in a magnetic contribution of $6x\mu_0$, and there are 8 Fe with 2 Ge atoms as NN which contribute with $8x\mu_2$, where $\mu_2 = 1.85\,\mu_B$/at. Thus, the magnetic contribution of a DO_3 cell can be calculated as

$$\mu_{cell} = \frac{122}{125}[5 \times 2.15 + 8 \times 1.7] + \frac{3}{125}[6 \times 2.15 + 8 \times 1.85]. \tag{8}$$

Considering the Fe and Ge mass we concluded that the magnetic contribution of the nanocrystals in the alloy was 144 ± 2 emu/g. The error was calculated considering the error carried from the Mössbauer analysis.

If we assume that $M_{nc} = cM_{cell} + (1-c)M_{am}$ (where c is the crystalline mass fraction, M_{nc} is the measured saturation magnetization of the nanocrystalline sample, M_{cell} is the calculated saturation magnetization of the cell and M_{am} is the remnant amorphous saturation magnetization) and considering that the crystalline mass fraction could be around 85% of the alloy, the magnetic contribution of the amorphous phase will be close to 117 emu/g.

4. Conclusions

The structural analysis allowed us to confirm that Ge stabilizes the nanocrystalline phase and delays boride precipitation. Mössbauer spectroscopy showed that after 1 h at 823 K the 87.7 at% of Fe atoms were in the crystalline phase. Consequently, the composition of α-Fe(Ge) nanograins remained at (18.6 ± 0.5) at% Ge and the amorphous matrix impoverished in Fe. Typical activation energy value for FINEMET alloy of 4.3 eV/at and Curie temperature of 664.0 K were obtained from DSC analysis. From magnetic measurement the material showed the softest magnetic properties between $T_{ann} = 673$ and 873 K with a minimum value of 5 A/m. Saturation magnetization of as-quenched and nanocrystalline samples was 138 ± 2 and 140 ± 4 emu/g, respectively. Considering the Fe and Ge masses we found that the magnetic contribution of the nanocrystals in the alloy was 144 ± 2 emu/g.

Acknowledgments

This work was supported by the Universidad de Buenos Aires, the Ministerio de Ciencia, Tecnología e Innovación Productiva and Comisión Nacional de Investigaciones Científicas y Tecnológicas (CONICET).

References

[1] Y. Yoshizawa, S. Oguma, K. Yamauchi, J. Appl. Phys. 64 (1988) 6044.
[2] K. Suzuki, A. Makino, N. Kataoka, A. Inoue, T. Masumoto, Mater. Trans. JIM 32 (1991) 93.
[3] A. Makino, T. Hatanai, Y. Naitoh, T. Bitoh, A. Inoue, T. Masumoto, IEEE Trans. Magn. 33 (1997) 3793.
[4] M.A. Willard, D.E. Laughlin, M.E. McHenry, D. Thoma, K. Sickafus, J.O. Cross, V.G. Harris, J. Appl. Phys. 84 (1998) 6773.
[5] G. Herzer, in: K.H.J. Buschow (Ed.), HandBook of Magetic Materials, 1997, p. 10.
[6] K. Hono, A. Inoue, T. Sakurai, Appl. Phys. Lett. 58 (1991) 2180.
[7] M.T. Clavaguera-Mora, N. CLavaguera, D. Crespo, T. Pradel, Prog. Mater. Sci. 47 (6) (2002) 559.
[8] J. Bigot, N. Lecaude, C.J. Perron, C. Milan, C. Ramiarinjaona, J.F. Rialliant, J. Magn. Magn. Mater. 133 (1994) 299.
[9] V. Cremaschi, G. Sánchez, H. Sirkin, Phys. B 354 (2004) 213.
[10] W. Lefebvre, S. Morin-Grognet, F. Danoix, J. Magn. Magn. Mater. 301 (2006) 343.

[11] M.E. McHenry, Prog. Mater. Sci. 44 (1999) 291.
[12] F. Alves, R. Lebourgeois, T. Waeckerle, Euro. Trans. Electr. Power 15 (2005) 467.
[13] R.A. Brand, Normos Program, Internal Report, Angewandte Physik, Universität Duisburg, 1987.
[14] G. Rixecker, P. Schaaf, U. Gonser, Phys. Stat. Sol. 139 (1993) 309.
[15] J.A. Moya, V.J. Cremaschi, H. Sirkin, Physica B 389 (2007) 159.
[16] M. Rubinstein, V.G. Harris, P. Lubitz, J. Magn. Magn. Mater. 234 (2001) 306.
[17] W.Z. Chen, P.L. Ryder, Mater. Sci. Eng. B 34 (1995) 204.
[18] D. Muraca, V.J. Cremaschi, H. Sirkin, J. Magn. Magn. Mater. 311 (2007) 618.
[19] G. Rixecker, P. Schaaf, U. Gonser, J. Phys. Condens. Matter 4 (1992) 10295.
[20] M. Miglierini, J. Phys. Condens. Matter 6 (1994) 1431.
[21] H. Kissinger, Anal. Chem. 29 (1957) 1702.
[22] A. Pratap, K.N. Lad, T. Lilly Shanker Rao, P. Majmudar, N.S. Saxena, J. Non-Cryst. Sol. 345 & 346 (2004) 178.
[23] G. Herzer, IEEE Trans. Magn. 26 (1990) 1397.
[24] H. Okumura, D.E. Laughlin, M.E. McHenry, J. Magn. Magn. Mater. 2 (2003).
[25] W. Brinton Corb, Phys. Rev. B 31–4 (1984) 2521, (67, 347).
[26] D. Muraca, V. Cremaschi, J. Moya, H. Sirkin, J. Magn. Magn. Mater. (2007), doi:10.1016/j.jmmm.2007.08.028.